Dynamic Light Scattering of Dilute Polymer Solutions in the Nonasymptotic q Region

Charles C. Han*

Center for Materials Research, Polymer Science and Standards Division, National Bureau of Standards, Washington, D.C. 20234

A. Ziya Akcasu

Department of Nuclear Engineering, The University of Michigan, Ann Arbor, Michigan 48109. *Received December 15, 1980*

ABSTRACT: Polystyrene solutions in the dilute region have been studied by dynamic light scattering experiments. The first cumulant, $\Omega(q)$, has been extracted consistently by either cumulant analysis or shape function analysis. It is found that $\Omega(q)$ approaches q^2 dependence for $qR_g \ll 1$ and q^3 dependence for $qR_g \gg 1$, with a broad transition region. It is also found that the magnitudes of the first cumulant in the q^3 region change as the solvent is changed from a Θ solvent to a good solvent. In both cases, experimental results agree better with theoretical calculations which use a preaveraged Oseen tensor.

Introduction

Conventionally, dynamic light scattering experiments in dilute polymer solutions are performed in the small q region characterized by $qR_g \ll 1$, where R_g is the radius of gyration. The primary purpose of these experiments, in which the intermediate scattering function $S(q,t)$ is obtained by photon correlation analysis, is to measure the translational diffusion coefficient by representing the $S(q,t)$ data as an exponential function and investigate its concentration and temperature dependence.[1] Dynamic light scattering can also be used, however, to study the internal motions of a polymer by adjusting the conditions of the experiment such that qR_g is comparable to or larger than unity. Since the maximum value of q is determined by the wavelength of the incident laser beam, this condition can only be satisfied by working with polymers of large molecular weights. For such values of qR_g, the shape of $S(q,t)$ deviates appreciably from a single exponential and makes the interpretation of the experiment more difficult. There have been attempts, with only partial success,[2-4] to measure the longest internal relaxation time of a molecule by representing $S(q,t)$ data as a superposition of two exponentials in the vicinity of qR_g near unity. In the intermediate q region defined by $qR_g \gg 1$ but $ql \ll 1$, where l is the statistical length, the interpretation of dynamic scattering experiments becomes once more straightforward. Dubois-Violette and de Gennes[5] showed in 1968 that the normalized $S(q,t)$ can be scaled as $S(q,t) \equiv \exp[f[\omega_c(q)t]]$ when f is expressed as a function of the dimensionless time $\tau \equiv \omega_c(q)t$, for all values of q in the above asymptotic region. They obtained the shape function $f(\tau)$ explicitly for an unperturbed Gaussian chain and found that the characteristic frequency $\omega_c(q)$ is proportional to $(k_BT/\eta_0)q^3$, where k_BT and η_0 denote the temperature and viscosity of the solvent. Dynamic light scattering experiments in the intermediate q region were first performed by Adam and Delsanti,[6] to check the power law dependence of the characteristic frequency. Experimentally, it is difficult to strictly satisfy the condition $qR_g \gg 1$ and $ql \ll 1$ for all q, as is required to check the validity of the asymptotic theory. Recently, Akcasu et al.[7] developed a method for the interpretation of dynamic scattering experiments, in terms of the first cumulant $\Omega(q)$ of $S(q,t)$, in all q regions, including the transition region where qR_g is allowed to vary from $qR_g \ll 1$ to $qR_g \gg 1$. The first cumulant is the initial slope of $S(q,t)$ and can be determined experimentally by cumulant analysis on the $S(q,t)$ data. The first cumulant has been calculated for all values of q and various chain models as a function of temperature. It is found that $\Omega(q)$ coincides with the characteristic frequency $\omega_c(q)$ in the intermediate q region and yields the short-time diffusion coefficient when $qR_g \ll 1$. Dynamic light scattering experiments which explore the transition q region by the above scheme of Akcasu et al. have been performed only very recently by Han,[7] Chu,[8] and Gulari and Alkhafji,[9] under a variety of experimental conditions.

The purpose of this paper is to present a systematic study in which we explore the q dependence of the first cumulant as a function of molecular weight in both good and Θ solvents. Results are compared to the theoretical predictions.

Table I

sample	$\bar{M}_w \times 10^{-6}$	$\bar{M}_w/\bar{M}_n$	c, mg/mL	solvent	η_0, cP
LF4	4.1	~1.1	0.16	toluene	0.566
			0.275	cyclohexane	0.75
F505	5.05	1.02	0.26	cyclohexane	0.75
F720	7.5	1.05	0.175	cyclohexane	0.75
F1300	13.4	1.17	0.24	cyclohexane	0.75
LF44	44.0	~1.1	0.18	toluene	0.566
			0.20	THF	0.46
			0.11	cyclohexane	0.75
PS48	48.0	1.3	0.22	toluene	0.566

Experimental Section

Six different polystyrene samples were used in this study. Samples LF4 and LF44 were kindly given to us by Professor L. Fetters of the University of Akron. Samples F505, F720, and F1300 were obtained from Toyo Soda Co. of Japan, and sample PS48 was obtained from Japan Synthetic Rubber Co. Molecular weights and the polydispersity ratio, $\bar{M}_w/\bar{M}_n$, are quoted in Table I. Also listed in Table I are concentrations and solvent viscosities used in this study. ACS spectrograde cyclohexane, THF, and toluene were used for preparing the solutions. All solutions were prepared by filtering solvent directly into clean glassware which contain preweighed polymers. Millipore filters with pore size 0.22 μm were used for cyclohexane and toluene filtration, but Millipore Teflon filters with pore size 0.2 μm were used for THF filtration. Cyclohexane solutions were kept at 40 °C and toluene as well as THF solutions were kept at room temperature for at least 24 h, with occasionally gentle shaking, before being used for scattering experiments.

All scattering experiments were carried out on a photon counting instrument with either a minicomputer-based correlator[10] or a Malvern 7025 correlator. The 4880-Å line from an Ar ion laser was used for the experiment. Cylindrical sample cells were used and mounted at the center of a temperature-controlled, refractive index matched bath goniometer. Temperatures were controlled at 35.0 ± 0.1 °C for polystyrene–cyclohexane measurements and uncontrolled but monitored to be 23.0 ± 0.2 °C for polystyrene–toluene and polystyrene–THF measurements.

The intermediate scattering function $S(q,t)$ is obtained from the experimental time correlation function $C(q,t)$ of the scattered light as[1]

$$C(q,t) = 1 + \beta S(q,t)^2 \quad (1)$$

with β as an adjustable parameter. This introduces an extra parameter in all data analysis, but this parameter will not be mentioned again for the sake of brevity.

Data Analysis

Two procedures can be followed to extract the first cumulant, $\Omega(q)$, from the $S(q,t)$ data.[7]

A. Cumulant Analysis. In this method $S(q,t)$ is represented[11] by $\exp[-\Omega t(1 + A_1 t + A_2 t^2 + ...)]$, and $\Omega(q)$ is determined by nonlinear regression analysis. It is also possible to fit $-\Omega t(1 + A_1 t + A_2 t^2 + ...)$ to $\ln S(q,t)$ data by linear regression analysis. Another possibility used in literature[12] is to represent $S(q,t)$ by $\exp(-\Omega t)[1 + B_1 t^2 + B_2 t^3]$. In our experiment we have used all three of these options to make sure that they yield consistent results for $\Omega(q)$ with the same data. Equal weights were used for all correlation data in the cumulant analysis. The number of terms in the cumulant expansion depends on the q region as well as the time range of the experiment. The criterion is that $\Omega(q)$ should become insensitive to the additional terms in the expansion. Our experience shows that even a single exponential yields sufficiently accurate estimates of $\Omega(q)$ if the time range of the experiment is restricted to values $\Omega t < 0.4$, where $S(q,t)$ decays approximately to $\exp(-0.4) = 0.67$ of its original value. When the experimental time range is increased, the single-exponential fit fails, as expected, and one needs full cumulant analysis. We found that all three forms of the cumulant analysis still yield consistent results for $\Omega(q)$ with three or more terms in the q region, $qR_g \leq 2$ and $\Omega t \lesssim 1$. For larger values of qR_g, particularly in the intermediate q region, more terms are needed and the precision of the results becomes very poor. In this q region, we feel that the shape function analysis yields more precise results if it is available. When the shape function is not available, such as in the good-solvent case, we still use three- or four-term cumulant fits, keeping the time range (with truncation of correlation data if necessary) to $\Omega t < 1$ rather than increasing the number of terms.

B. Shape Function Analysis. In this method $S(q,t)$ is represented as $\exp[f(\tau,qR_g)]$ for $ql \ll 1$, where $\tau = \Omega t$ and $f(\tau,qR_g)$ is the shape function. The latter is a slowly varying function of qR_g in the transition q region, where $qR_g \sim 1$, and becomes independent of qR_g in the intermediate q region as well as the small q region, where $qR_g \ll 1$. The variation of $f(\tau,qR_g)$ with τ for various values of qR_g in the case of a closed unperturbed Gaussian chain has been presented elsewhere.[7] The shape function $f(\tau,ql)$ for an open infinite chain is also available as a function of τ and ql.[7] In the limit $ql \to 0$ (or $qR_g \to \infty$ in the previous case) we obtain the asymptotic shape function $f(\tau)$ appropriate for the intermediate q region[5,7] as

$$S(q,t) = \int_0^\infty du \exp\{-u - (\Omega t)^{2/3} h[u(\Omega t)^{-2/3}]\}$$

where

$$h(u) \equiv (2/\pi) \int_0^\infty dx \, (\cos xu/x^2)[1 - \exp(-x^{3/2}/2^{1/2})] \quad (2)$$

A nonlinear regression routine[13] was used for fitting data to eq 2.

Figure 1 shows the experimental $S(q,t)$ of sample LF44 at $qR_g = 6.4$ under Θ conditions in the time range up to 520 μs with a delay time of 5 μs. We observe that the accuracy of the data beyond $t = 440$ μs becomes increasingly poor because $S(q,t)$ decays well below the noise level. The maximum time range in a dynamic light scattering experiment is, in general, restricted by the noise level. The dashed curve in Figure 1 represents the asymptotic shape function which is fitted to the experimental points with $\Omega = 8.14 \times 10^3$ s^{-1}. We also fitted the data to a single exponential and obtained $\Omega = 5.98 \times 10^3$ s^{-1} to demonstrate the inadequacy of a single-exponential representation in this time range.

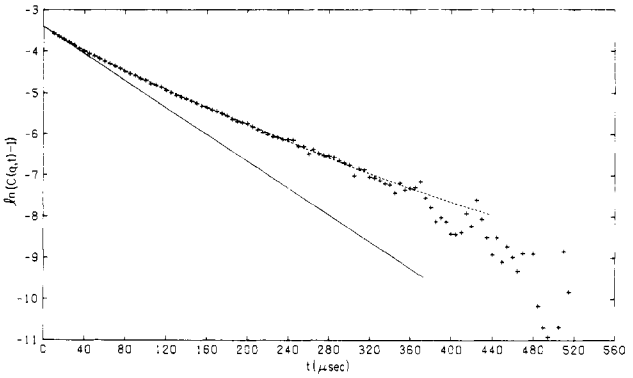

Figure 1. Experimental correlation data of LF44 in cyclohexane at a scattering angle $\theta = 120°$ with a delay time of 5 μs. The dashed curve is the best fit by using the asymptotic shape function and the solid line is the corresponding initial slope.

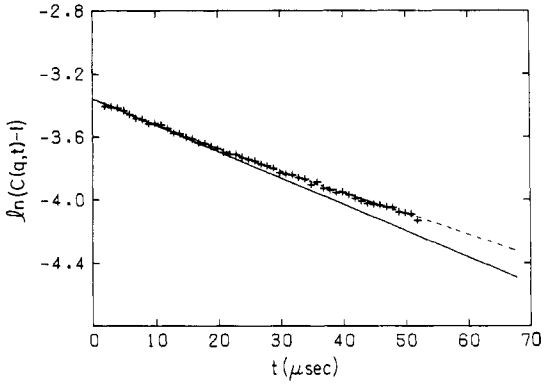

Figure 2. Correlation data with experimental conditions identical to those of Figure 1 except with 1-μs delay time. Again, the dashed curve is the best asymptotic shape function fit and the solid line is the corresponding initial slope.

Figure 2 shows the decay of $S(q,t)$ for the same qR_g and identical conditions except for a smaller time range of 1–50 μs and a 1-μs delay time. The asymptotic shape function fit yielded in this case $\Omega = 8.34 \times 10^3$ s^{-1}, which is within 2.5% of the previous result. The single-exponential fit in this range yields 8.01×10^3 s^{-1}, which is only 5% less than a correct value. In general, a single-exponential representation always underestimates $\Omega(q)$. The point here is that $\Omega(q)$ can be extracted from $S(q,t)$ data with reasonable accuracy if the purpose of the experiment is only to determine $\Omega(q)$ by a simple exponential fit, provided the time range of the experiment is sufficiently small, e.g., $\Omega t \leq 0.4$. However, if the purpose of the experiment is also to investigate the shape of $S(q,t)$ as a function of time in order to verify theoretical model calculations, then the time range of the experiment should be extended as much as possible, provided $S(q,t)$ is above the noise level.

We extracted $\Omega(q)$ from data obtained under Θ conditions by cumulant analysis when $qR_g \leq 2$ and by shape function analysis, using the asymptotic shape function, when $qR_g \geq 2$. Actually, the shape function attains its asymptotic form, according to the exact closed-chain calculations presented in ref 7, when $qR_g \geq 4$. We have

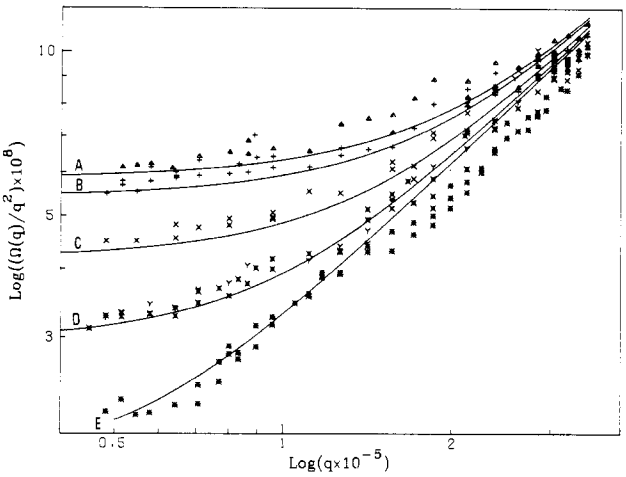

Figure 3. Variation of the first cumulant as a function of q for five different polystyrene samples in cyclohexane as listed in Table I. Solid lines are calculated from eq 4 with $lN^{1/2}$ end-to-end distances (A) 1.95×10^{-5}, (B) 2.11×10^{-5}, (C) 2.74×10^{-5}, (D) 3.90×10^{-5}, and (E) 6.80×10^{-5} cm, just to illustrate the analytical trends. The values of $lN^{1/2}$ are adjusted for crude agreement.

not distinguished between the asymptotic shape function and the actual one corresponding to a particular qR_g for $qR_g \geq 2$ to avoid lengthy calculations involved in obtaining the shape function for each qR_g. The use of the asymptotic shape function for all $qR_g \geq 2$ underestimates $\Omega(q)$ slightly in the range $qR_g = 2$–4, with the maximum inaccuracy being less than ~5% at $qR_g = 2$ and decreasing when qR_g becomes larger. We have calculated R_g by using

$$R_g = 3 \times 10^{-9} M^{1/2} \text{ cm} \tag{3}$$

instead of obtaining it self-consistently from $S(q,t)$ data and $\Omega(q)$ with the iteration procedure suggested in ref 7. This is because we want to investigate the q dependence of $\Omega(q)$ without any adjustable parameter, provided that $\Omega(q)$ can be extracted as described above.

In the case of good-solvent data we used cumulant analysis to extract $\Omega(q)$ for all values of qR_g to avoid the question of using the shape function calculated under Θ conditions. The asymptotic shape function in good solvent is not available analytically although it is not expected to deviate appreciably from that in Θ solvent, as concluded by Delsanti.[14]

The values of $\Omega(q)$ as extracted from the $S(q,t)$ are presented in Figure 3 as a function of q for various molecular weights.

Interpretation and Discussion

We calculated $\Omega(q)$ by using

$$\frac{\Omega(q)}{q^2 D_\nu} = \frac{(1-\nu)(2-\nu)}{2} \kappa_\nu \frac{\gamma\left(\frac{1-\nu}{2\nu}, \kappa_\nu^2\right) - \kappa_\nu^{-1/\nu}\gamma\left(\frac{2-\nu}{2\nu}, \kappa_\nu^2\right)}{\gamma\left(\frac{1}{2\nu}, \kappa_\nu^2\right) - \kappa_\nu^{-1/\nu}\gamma\left(\frac{1}{\nu}, \kappa_\nu^2\right)} \tag{4}$$

where

$$\kappa_\nu^2 \equiv (qR_g)^2(1+\nu)(1+2\nu)/3$$

$$R_g \equiv lN^\nu [2(1+\nu)(1+2\nu)]^{-1/2}$$

$$D_\nu = \frac{k_B T}{\eta_0 R_g} \frac{[3\pi(1+\nu)(1+2\nu)]^{-1/2}}{\pi(1-\nu)(2-\nu)}$$

and where $\gamma(\mu,x)$ denotes the incomplete gamma function

$$\gamma(\mu,x) \equiv \int_0^x dt\, t^{\mu-1} \exp(-t)$$

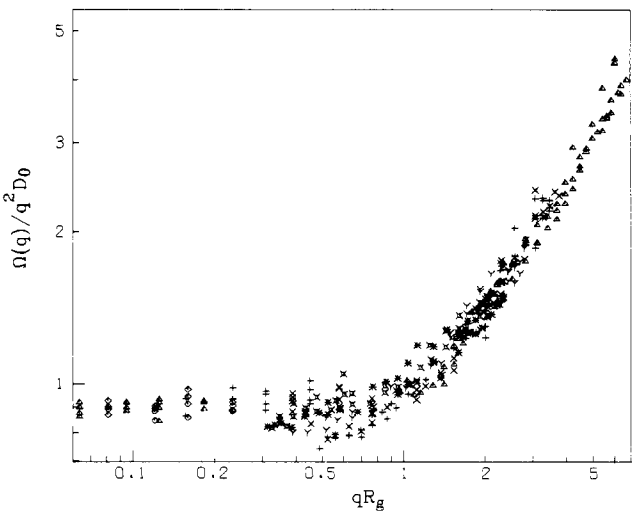

Figure 4. Variation of $\Omega(q)/q^2 D_0$ as a function of qR_g at the Θ condition without concentration correction.

This expression yields $\Omega(q)$ for Θ conditions when $\nu = 1/2$ and for good-solvent conditions when $\nu = 3/5$. It was obtained by Akcasu et al.,[15] using a preaveraged Oseen tensor for a single Gaussian chain and replacing summation in the original expression of $\Omega(q)$ by integration. D_ν reduces to the diffusion coefficient in Kirkwood's approximation when $\nu = 1/2$. It is observed that $\Omega(q)/q^2 D_\nu$ depends only on qR_g. In the limit $qR_g \to 0$, it yields $\Omega(q) \to q^2 D_\nu$. When $qR_g \to \infty$, i.e., in the intermediate q region, it yields

$$\frac{\Omega(q)}{(k_B T/\eta_0) q^3} = \frac{\Gamma[(1-\nu)/2\nu]}{\Gamma(1/2\nu)(6\pi)\pi^{1/2}} \tag{5}$$

where $\Gamma(x)$ is the usual gamma function. The right-hand side is the value of the plateau in the q^3 region, which yields $1/6\pi$ with $\nu = 1/2$ in Θ solvent and 0.071 with $\nu = 3/5$ in good solvent. The solid lines in Figure 3 denote the theoretical $\Omega(q)$ as calculated from eq 4 with $\nu = 1/2$ and lN^ν values as indicated.

In Figure 4, we have presented the normalized data $\Omega(q)/q^2 D_0$ as a function of qR_g to demonstrate that a reduced curve predicted by eq 4 and also by eq 7 below can be obtained. In this plot $D_0 = 0.195 k_B T/\eta_0 6^{1/2} R_g$ was used, with R_g calculated from eq 3. It should be pointed out that values of $\Omega(q)/q^2 D_0$ are less than one at small qR_g. This deviation reflects the discrepancy between D_0 and the true diffusion coefficient and is larger than the sum of the concentration correction discussed below and the D_1 correction arising from the distinction between short- and long-time diffusion coefficients.[17]

In Figure 5 we have plotted $\Omega(q)/q^3(k_B T/\eta_0)$ as a function of qR_g to demonstrate the independence of this ratio of the molecular weight when it is expressed as a function of qR_g. We observe that the data are consistently below the theoretical prediction. The agreement improves somewhat when the data are corrected for the concentration dependence. In the small q region, where $\Omega(q) \to q^2 D(c)$, the concentration correction is made according to[18]

$$D(c) = D(0) - 7.76 \times 10^{-9} c \tag{6}$$

where c is the concentration in mg/mL. The coefficient of c is independent of the molecular weight in Θ solvents as shown both theoretically[19–21] and experimentally.[18,22,23] For cyclohexane $D(0) = 1.39 \times 10^{-4} M^{-1/2}$ cm²/s. The concentration in our experiments was between 0.1 and 0.3

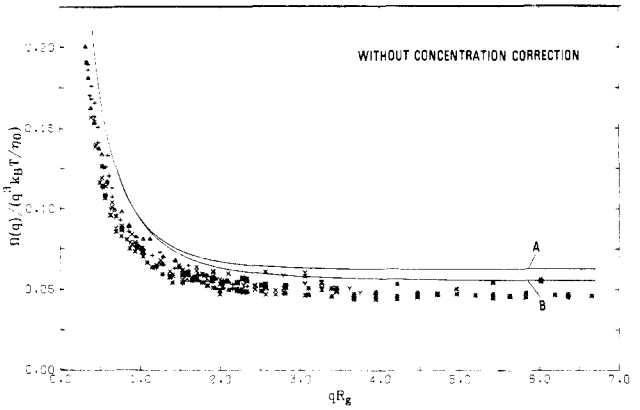

Figure 5. Variation of the reduced first cumulant $\Omega(q)/(q^3k_BT/\eta_0)$ as a function of qR_g at the Θ condition without concentration correction. Curve A is calculated according to eq 7 without preaveraging the Oseen tensor and curve B is calculated according to eq 4 with preaveraging the Oseen tensor.

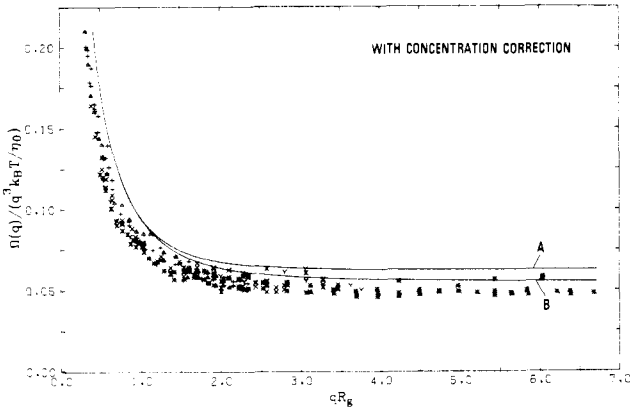

Figure 6. Variation of the reduced first cumulant as a function of qR_g at the Θ condition with concentration correction. Curves A and B are the same as in Figure 5.

mg/mL so $D(0)$ is about 3.1% larger than the measured value of $D(c)$ when $M = 4.1 \times 10^6$ and 4.1% when $M = 4.4 \times 10^6$. The data points in Figure 5 must be increased by $D(0)/D(c)$ in the small q region to account for the finite concentration. There is not established theoretical prediction for the concentration dependence of the first cumulant in the transition and intermediate q regions. We therefore shifted the data upward uniformly for all q values in Figure 6. The data are still consistently below the theoretical prediction although the agreement is improved. Considering the uncertainties in the extraction of $\Omega(q)$ from $S(q,t)$ data, the agreement may be regarded as satisfactory. We note that the agreement would be further improved for $qR_g \leq 1.5$ if the value of R_g were adjusted.

The expression of $\Omega(q)$ in eq 4 was obtained by using the preaveraged Oseen tensor. Recently, Benmouna and Akcasu[24] calculated $\Omega(q)$ without preaveraging the Oseen tensor as (eq 6 in ref 24 contains misprints)

$$\Omega(q)/q^2D_\nu = [3(1-\nu)(2-\nu)/16\nu]\kappa_\nu^{1-1/\nu} \times \left[\int_0^1 du\ (1-u)e^{-u^{2\nu}\kappa_\nu^2}\right]^{-1} \int_0^{\kappa_\nu^2} du\ (1-u^{1/2\nu}/\kappa_\nu^{1/\nu})u^{1/2\nu-2} \times \left[-u^{-1/2} + (2+u^{-1})e^{-u}\int_0^{u^{1/2}} dt\ e^{t^2}\right] \quad (7)$$

where D_ν, κ_ν, and R_g have the same meaning as in eq 4. This result is valid for both Θ and good solvents with $\nu = {}^1/_2$ and $\nu = {}^3/_5$, respectively. It yields again $\Omega(q) \to q^2D_\nu$ as $qR_g \to 0$. In the intermediate q region, where $qR_g \to \infty$, one finds

$$\frac{\Omega(q)}{q^3k_BT/\eta_0} = \frac{1}{(8\pi)\pi^{1/2}}\frac{J(\nu)}{\Gamma(1/2\nu)} \quad (8a)$$

where

$$J(\nu) \equiv \int_0^\infty du\ u^{1/2\nu-2}\left[-u^{-1/2} + (2+u^{-1})e^{-u}\int_0^{u^{1/2}} dt\ e^{t^2}\right] \quad (8b)$$

In the case of Θ solvent, eq 8b yields[24,25] $J(1/2) = \pi\pi^{1/2}/2$ so that the value of the plateau becomes ${}^1/_{16} = 0.0625$ instead of $1/6\pi = 0.053$, obtained with the preaveraged Oseen tensor. In the good-solvent limit $J(3/5)$ has been evaluated numerically[24] as $J(3/5) = 3.965$. The latter yields the plateau value 0.079 in eq 8a, instead of 0.071 obtained with the preaveraged Oseen tensor.

In Figures 5 and 6, we have also plotted $\Omega(q)/q^3(k_BT/\eta_0)$, using eq 7 with $\nu = {}^1/_2$. (Actually, for computational convenience, we used the original form of eq 7, in which the summations are not replaced by integrals, i.e., eq 3 of ref 21.) It is observed that preaveraging does not affect the behavior of this ratio for small qR_g but decreases it by about 15% in the plateau region. The data seem to be in better agreement with the theoretical predictions with the preaveraged Oseen tensor. We have no explanation for this observation.

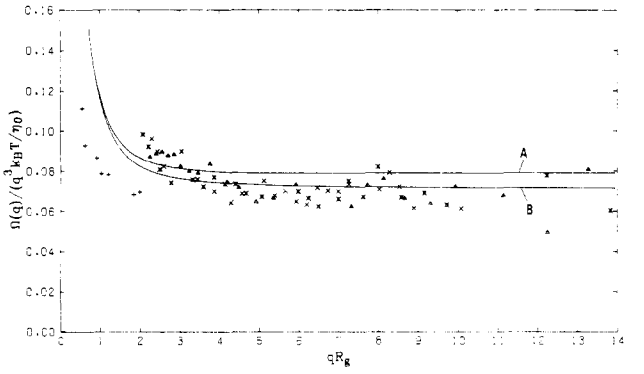

Figure 7. Variation of the reduced first cumulant as a function of qR_g in good solvents. Curves A and B are the same as in Figure 5, except $\nu = 0.6$.

Figure 7 represents both the experimental and theoretical results in the case of good solvent. The data in this case have not been corrected for concentration. Again preaveraging provides a better agreement with the data. The increase in the plateau value from Θ to good solvent seems now to be firmly established as a trend.

In conclusion, the dynamic light scattering experiments in the transition region as well as in the asymptotic q region seem to be interpretable on the basis of the first cumulant[7] very satisfactorily as far as trends are concerned but somewhat less satisfactorily with respect to quantitative agreement.

Acknowledgment. We gratefully acknowledge stimulating discussions with Drs. I. C. Sanchez, E. A. DiMarzio, C. M. Guttman, and F. L. McCrackin at the National Bureau of Standards. Acknowledgment is also made to donors of the Petroleum Research Fund, administered by the American Chemical Society, for partial support of A.Z.A.

References and Notes

(1) For example: Chu, B. "Laser Light Scattering"; Academic Press: New York, 1974.

(2) Pecora, R. *J. Chem. Phys.* **1965**, *43*, 1562. *Ibid.* **1968**, *49*, 1032.
(3) Huang, W. N.; Frederick, J. E. *Macromolecules* **1974**, *7*, 34.
(4) Jones, G.; Caroline, D. *Chem. Phys.* **1979**, *37*, 187.
(5) Dubois-Violette, E.; de Gennes, P. G. *Physics* **1967**, *3*, 181.
(6) Adam, M.; Delsanti, M. *Macromolecules* **1977**, *10*, 1229.
(7) Akcasu, A. Z.; Benmouna, M.; Han, C. C. *Polymer* **1980**, *21*, 866.
(8) Nose, T.; Chu, B. *Macromolecules* **1979**, *12*, 1122.
(9) Gulari, E.; Alkafaji, S., private communication.
(10) Han, C. C. *Rev. Sci. Instrum.* **1978**, *49*, 31.
(11) Koppel, D. E. *J. Chem. Phys.* **1972**, *57*, 4814.
(12) Brown, J. C.; Pusey, P. N. *J. Chem. Phys.* **1975**, *62*, 1136.
(13) Ryshpan, J. NREG routines; Academic Computing Center, The University of Wisconsin, Madison: Madison, Wisc., 1972.
(14) Delsanti, M. Thesis, Université de Paris-sud, 1978.
(15) Benmouna, M.; Akcasu, A. Z. *Macromolecules* **1978**, *11*, 1187.
(16) Akcasu, A. Z.; Gurol, H. *J. Polym. Sci., Polym. Phys. Ed.* **1976**, *14*, 1.
(17) See, for example: (i) Note in ref 7. (ii) Hortz, A.; Fixman, M. *J. Am. Chem. Soc.* **1968**, *90*, 3048. (iii) Zimm, B. H. *Macromolecules* **1980**, *13*, 592.
(18) Han, C. C. *Polymer* **1979**, *20*, 259.
(19) Pyun, C. W.; Fixman, M. *J. Chem. Phys.* **1964**, *41*, 937.
(20) Yamakawa, H. "Modern Theory of Polymer Solutions"; Harper and Row: New York, 1971.
(21) Akcasu, A. Z.; Benmouna, M. *Macromolecules* **1978**, *11*, 1193.
(22) Han, C. C.; Akcasu, A. Z. *Polymer*, in press.
(23) Gulari, E.; Gulari, E.; Tsunashima, Y.; Chu, B. *Polymer* **1979**, *20*, 347.
(24) Benmouna, M.; Akcasu, A. Z. *Macromolecules* **1980**, *13*, 409.
(25) Burchard, W.; Schmidt, M.; Stockmayer, W. H. *Macromolecules* **1980**, *13*, 580.

Composition and Fractionation within Conjugated Isotropic and Anisotropic Phases of Lyotropic Liquid Crystals

G. Conio, E. Bianchi, A. Ciferri,* and A. Tealdi

Centro Studi Macromolecole, Istituto di Chimica Industriale, University of Genoa, Genoa, Italy. *Received December 30, 1980*

ABSTRACT: The composition of conjugated isotropic and anisotropic phases occurring for solutions of poly(*p*-benzamide) in *N,N*-dimethylacetamide–LiCl was investigated. The phases were separated by ultracentrifugation, preferably following the nucleation of the isotropic phase by dilution of a pure anisotropic solution. The study included the determination of the molecular weight (through intrinsic viscosity) of the solute within the two phases. A selective enrichment of high and low molecular weight species occurred in the anisotropic and isotropic phases, respectively. The solute molecular weight in the anisotropic phase increased as the volume fraction of the isotropic phase was increased. The efficiency of a refractionation process performed by diluting a pure anisotropic phase isolated from the biphasic region was demonstrated. The compositions of isolated isotropic and anisotropic phases were found to decrease with the volume fraction of isotropic phase. The above results are discussed in terms of recent theoretical treatments of polydisperse rodlike molecules. Extremely clear patterns of the nematic order were obtained as a result of fractionation and separation of the isotropic phase.

In a solution of rodlike particles above a critical solute concentration C_p^*, a transformation from an isotropic to an anisotropic phase is experimentally observed.[1-6] However, the two phases coexist in a discrete range of solute concentration. The amount of anisotropic phase grows at the expense of the isotropic one when the concentration is increased from C_p^* to a value C_p^{**}, above which only the anisotropic phase is stable.

A theory developed for monodisperse particles[7] produced a composition–temperature phase diagram which indicates the boundaries of the biphasic region for a given axial ratio x. According to this theory, the C_p^* and C_p^{**} values are the limiting compositions of the pure isotropic and anisotropic phases, respectively, and also the compositions of the coexisting phases within the biphasic region, irrespective of the relative amount of the two phases. Calculations show that this theory yields an approximate expression for the critical volume fraction of the solute in terms of the axial ratio, $v_2^* \simeq (8/x)(1 - 2/x)$. However, this approximation is satisfactory only in athermal solvents.

The experimental determination of C_p^* and C_p^{**} has been performed[1-6] by techniques supposedly sensitive to the first appearance of the anisotropic phase and to the complete disappearance of the isotropic one, respectively. However, reservations about the reliability of some techniques (particularly the viscometric one)[5,6,8] and about the attainment of true equilibrium[5] have recently been made. In particular, Matheson[8] has analyzed theoretically the steady flow viscosity of solutions of rodlike macromolecules in the entire range of polymer concentration. His results indicate that the nucleation of the anisotropic phase occurs at a lower concentration than that indicated by the maximum in the viscosity–concentration plot. This result is in line with recent experimental findings.[5,6] Moreover, all studies performed so far have involved polydisperse rigid polymers. For the latter, preliminary experimental results, as well as theory,[9] indicate a selective partitioning of low and high molecular weight components between the coexisting phases. Actually, the latter theory[9] predicts boundaries of the biphasic region which are strikingly different from the ones predicted by the earlier theory[7] valid for monodisperse systems.

Thus, from both the experimental and theoretical point of view, the need arises for a renewed and more sophisticated attempt to determine the parameters affecting the boundaries of the biphasic region. In this paper we have followed the approach of isolating the coexisting phases and determining their equilibrium composition and molecular weight partition. It will be shown that both parameters are strongly affected by the ratio of phase volumes. We have used the poly(*p*-benzamide)–*N,N*-dimethylacetamide/LiCl systems used in previous investigations.[5]

Experimental Section

Materials and Solutions. The poly(*p*-benzamide) (PBA) sample used in this investigation was kindly supplied by Dr. J.

0024-9297/81/2214-1084$01.25/0